Electronic Supplementary Material (ESI) for Molecular Systems Design & Engineering.
This journal is © The Royal Society of Chemistry 2021

Supplementary Material for on-line publication only

Formic Acid Dehydrogenation over Single Atom Pd-Deposited Carbon Nanocones for Hydrogen Production: Mechanistic DFT Study

Nuttapon Yodsin and Siriporn Jungsuttiwong*

Center for Organic Electronic and Alternative Energy, Department of Chemistry and Center for Innovation in Chemistry, Faculty of Science, Ubon Ratchathani University, Ubon Ratchathani 34190, Thailand.

**Corresponding author. E-mail: siriporn.j@ubu.ac.th (S.J.)*

Contents

Figure S20 H_2, CO_2, CO, and H_2O production as a function of temperature during FA decomposition via a) dehydrogenation and b) dehydration mechanisms on an Pd/dCNC catalyst.

Table S1 – Binding energies (E_{bind}) and structural properties of a Pd atom supported on the vacancy of CNC.

Table S2 – Gas adsorption properties of a Pd atom supported on different cone layers

Table S3 – *trans*-HCOOH adsorption properties of aи Pd atom supported dCNC

Table S4 – *cis*-HCOOH adsorption properties of a Pd atom supported dCNC

Table S5 – CO_2 and H_2 adsorption properties of a Pd atom supported dCNC

S1. The stability of the Pd atom on various cone layers

We optimized the geometry of Pd-doped dCNC on various cone layers to gain a suitable structure for further calculations. There are three possible structures, labeled dCNC-2L, dCNC-3L, and dCNC-4L (**Figure S1**). The dCNC cluster models consist of 53, 79, and 109 carbon atoms for Pd/dCNC-2L, Pd/dCNC-3L, and Pd/dCNC-4L, respectively. As illustrated in **Table S1**, the binding energies of each model are obtained to understanding the stability of the Pd atom on dCNC. The results showed that the binding energies of Pd atom over dCNC-2L, dCNC-3L, and dCNC-4L are -6.84, -6.86, and -6.85 eV, respectively. The bond length between Pd and its three neighboring C atoms are in agreement with reliable Pd/dCNC-4L model. For the electronic properties, the NBO charge on Pd is positive. and on the C atom is negative, confirming the electron transfer from Pd to the CNC support. The reaction gas (HCOOH) is expected to be very attractive with a strong interaction because of the more positive charge on the Pd atom in Pd/dCNC. Therefore, the deposited Pd atoms is pretended to be Lewis acid and it is expected to interact strongly with FA during dehydrogenation. From these results, the Pd atom can stably adsorbs with the large binding energies of all three case.

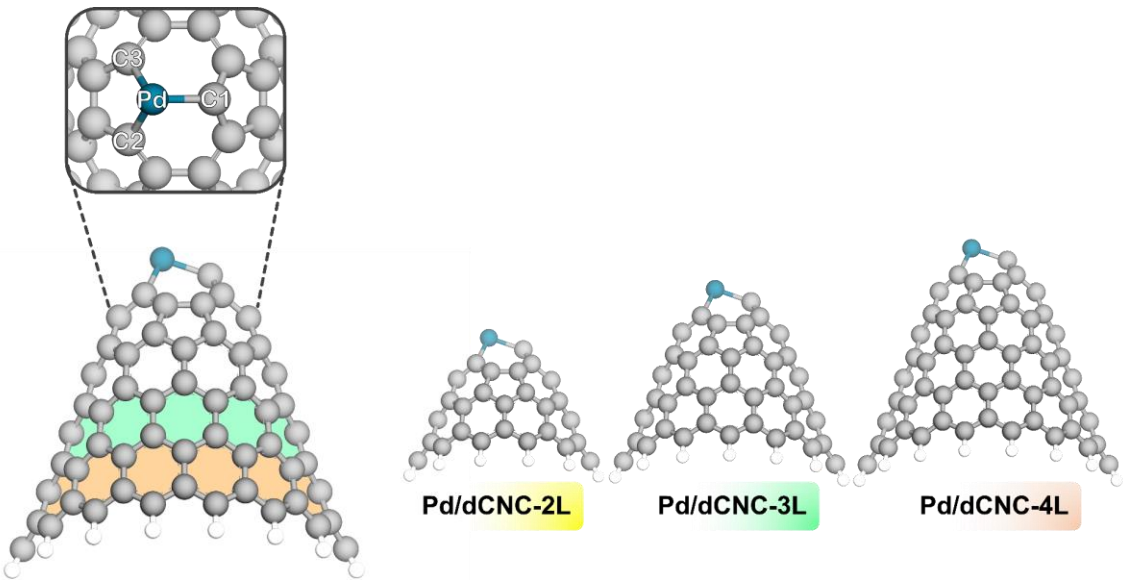

Figure S1 – Optimized Pd/dCNC cone length structures. Single Pd atom dopes the single vacancy in each cone.

Table S1 – Binding energies (E_{bind}) and structural properties of a Pd atom supported on the vacancy of CNC.

System	Number of C	E_{bind}, eV	d(Pd-C), Å	q(Pd)	q(C1, C2, C3)
Pd-*v*GP[1]	32	-5.37	1.96, 1.96, 1.96	N/A	N/A
Pd-*v*GP[2]	48	N/A	1.96, 1.96, 2.05	Pd -> C (0.4*e*-)	
Pd-dCNC-2L	53	-6.84	1.946, 1.985, 1.985,	0.517	-0.159, 0.001, 0.001
Pd-dCNC-3L	79	-6.86	1.948, 1.983, 1.983,	0.523	-0.156, 0.004, 0.004
Pd-dCNC-4L	109	-6.85	1.949, 1.983, 1.983,	0.524	-0.155, 0.005, 0.005

Note: *v*GP is vacancy graphene.

Stability of Pd atom over Pd/dCNC-2L

Figure S2 shows the suitable optimized structure of Pd/dCNC. We obtain the Pd/dCNC stability in terms of binding energy and structural parameters, as showed in **Table S1**. Our reliable results illustrate that the binding energy of a single Pd atom depositing on dCNC-2L is -6.83 eV, which is greater than Pd on graphene (-5.37 eV).[1] The metal forming clusters, migrating, and accumulating can prevent by these strong binding energy. Therefore, the Pd atom adsorbs to form a stable structure in Pd/dCNC material. Moreover, the structural properties are also observed. The bond lengths between Pd and its three neighboring C atoms are 1.946, 1.985, and 1.985 Å for Pd-C1, Pd-C2, and Pd-C3, respectively, which is in line with previous work.[1, 2] We found electron transferring from Pd to the CNC support confirming by the NBO analysis, which Pd is positive and on the C atom is negative.

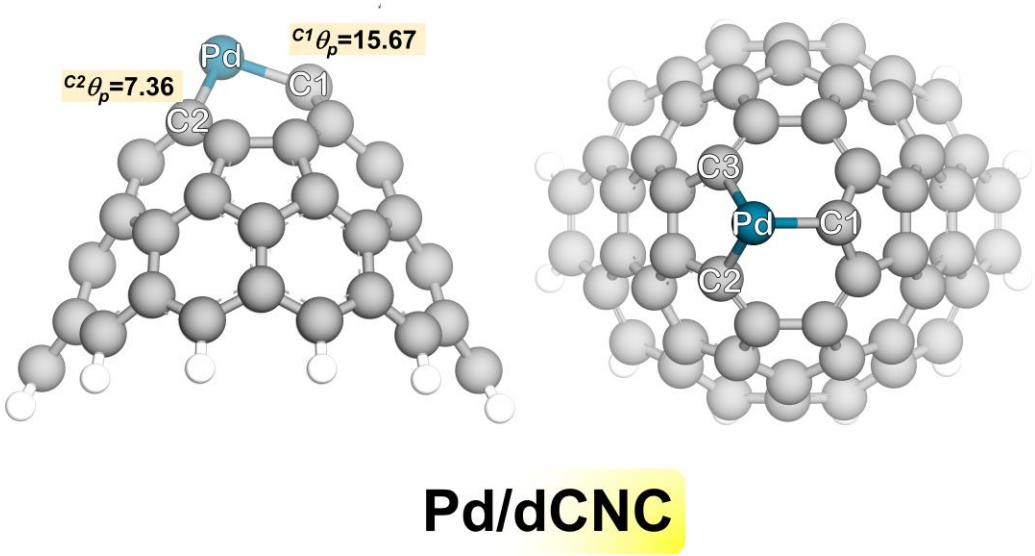

Figure S2 – Optimized structure for a Pd atom decorating a single vacancy CNC with the calculated θ_p of C1 and C2 (POAV analysis).

S2. The gas adsorption over Pd atom on various cone layers

The reaction mechanism of FA dehydrogenation starts with FA adsorption step. To gain the suitable model, we investigated the comparison on adsorption of the reaction gas (HCOOH, CO_2, and H_2) on different cone layers. The adsorption properties are discussed in the following sections.

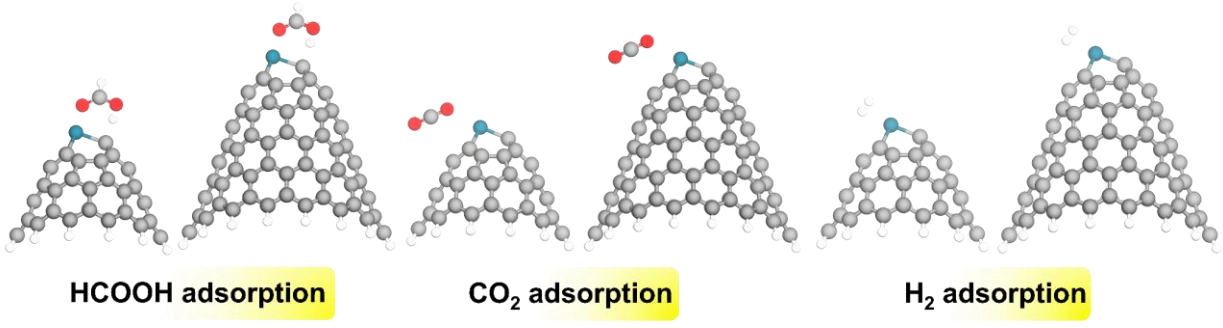

Figure S3 – Adsorption structures of HCOOH, CO_2, and H_2 on different cone layers

Table S2 – Gas adsorption properties of a Pd atom supported on different cone layers

System	E_{ads}, eV	*d*(gas-Pd), Å	*d*(Pd-C), Å	*q*(Pd)	*q*(gas)	*q*(C1, C2, C3)
HCOOH-Pd-dCNC-2L	-1.23	1.666, 2.204	2.061, 1.973, 1.992	0.558	0.037	-0.252, -0.024, 0.039
HCOOH-Pd-dCNC-4L	-1.23	1.699, 2.207	2.061, 1.972, 1.990	0.559	0.050	-0.249, -0.021, 0.042
CO_2-Pd-dCNC-2L	-0.42	2.469	1.970, 1.994, 1.994	0.494	0.080	-0.180, 0.008, 0.008
CO_2-Pd-dCNC-4L	-0.43	2.465	1.973, 1.993, 1.993	0.502	0.082	-0.175, 0.013, 0.013
H_2-Pd-dCNC-2L	-0.32	2.008	1.980, 2.015, 2.015	0.356	0.101	-0.172, 0.033, 0.032
H_2-Pd-dCNC-4L	-0.31	2.012	1.981, 2.013, 2.013	0.367	0.103	-0.169, 0.035, 0.035

Here, we studied on the involved gas reaction for clarify the fit model for the mechanism study. Form the results, we found either structural or electronic properties of the three different cone layers are not significantly different. So, we endeavor to use the suitable Pd/dCNC-2L for further study.

S3. The FA adsorption over Pd/dCNC-2L

Next, we studied all possible configurations of either *cis*- or *trans*-FA adsorption on Pd/dCNC surface. There are nine possible configurations for *trans*-FA and ten configurations for *cis*-FA as showed in **Figure S4** and **Figure S5**.

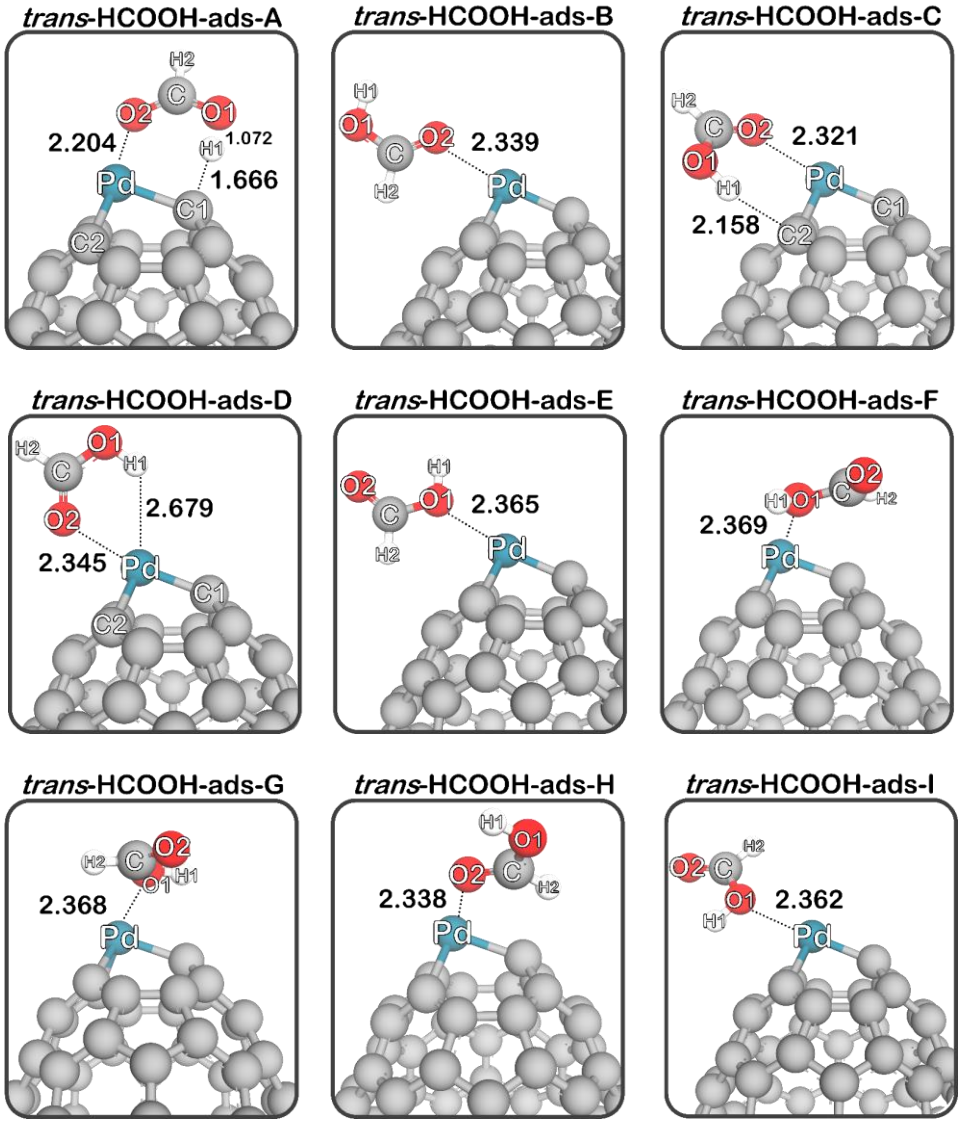

Figure S4 – All stable configurations of *trans*-HCOOH adsorption over Pd/dCNC

Table S3 – *trans*-HCOOH adsorption properties of a Pd atom supported dCNC

System	E_{ads}, eV	*d*(FA-Pd), Å	*d*(Pd-C), Å	*q*(Pd)	*q*(FA)	*q*(C1, C2, C3)
trans-HCOOH-ads-A	-1.23	1.666, 2.204	2.061, 1.973, 1.992	0.558	0.037	-0.252, -0.024, -0.046
trans-HCOOH-ads-B	-0.87	2.339	1.974, 2.001, 2.001	0.513	0.137	-0.202, 0.020, 0.019
trans-HCOOH-ads-C	-0.98	2.158, 2.321	1.975, 2.005, 2.009	0.505	0.138	-0.199, -0.073, 0.039
trans-HCOOH-ads-D	-0.77	2.345, 2.679	1.960, 2.004, 2.006	0.344	0.145	-0.180, 0.040, 0.040

trans-HCOOH-ads-E	-0.62	2.365	1.967, 2.002, 2.001	0.467	0.112	-0.188, 0.016, 0.018
trans-HCOOH-ads-F	-0.58	2.369	2.012, 1.990, 1.982	0.503	0.109	-0.161, -0.008, -0.013
trans-HCOOH-ads-G	-0.59	2.368	2.017, 1.993, 1.979	0.502	0.109	-0.170, -0.007, -0.013
trans-HCOOH-ads-H	-0.83	2.338	2.017, 1.997, 1.985	0.535	0.133	-0.170, 0.017, -0.021
trans-HCOOH-ads-I	-0.60	2.363	1.966, 2.000, 1.998	0.466	0.113	-0.190, 0.010, 0.019

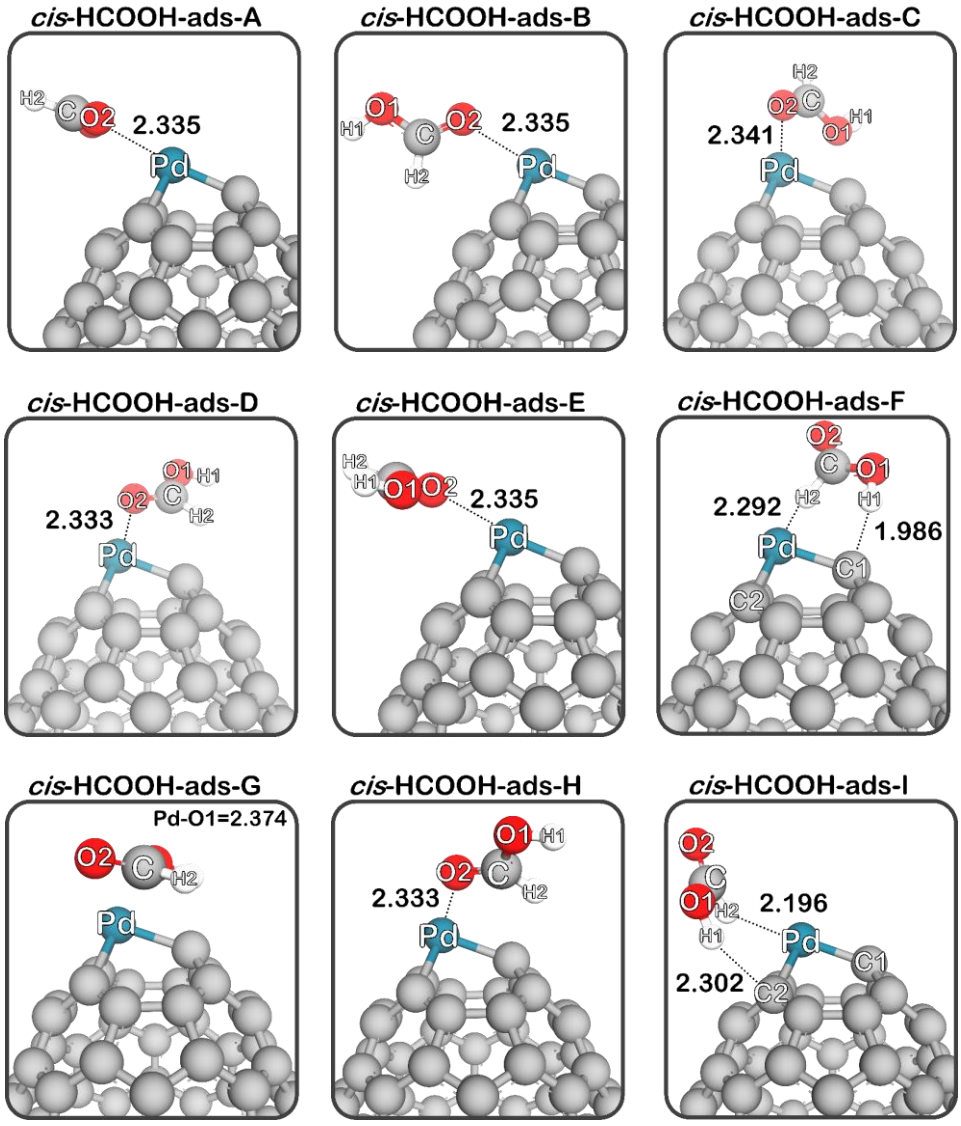

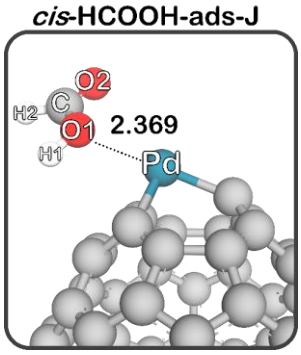

Figure S5 – All stable configurations of *cis*-HCOOH adsorption over Pd/dCNC

Table S4 – *cis*-HCOOH adsorption properties of a Pd atom supported dCNC

System	E_{ads}, eV	*d*(FA-Pd), Å	*d*(Pd-C), Å	*q*(Pd)	*q*(FA)	*q*(C1, C2, C3)
cis-HCOOH-ads-A	-0.86	2.335	1.973, 2.002, 2.002	0.490	0.136	-0.198, 0.038, 0.033
cis-HCOOH-ads-B	-0.92	2.335	1.975, 2.001, 2.001	0.526	0.138	-0.202, 0.019, 0.019
cis-HCOOH-ads-C	-0.78	2.341	2.017, 1.983, 2.000	0.521	0.136	-0.139, -0.011, 0.010
cis-HCOOH-ads-D	-0.90	2.333	2.018, 1.985, 1.998	0.546	0.134	-0.174, -0.021, 0.022
cis-HCOOH-ads-E	-0.86	2.335	1.973, 2.002, 2.002	0.490	0.136	-0.198, 0.033, 0.038
cis-HCOOH-ads-F	-0.51	1.986, 2.292	2.015, 1.986, 1.988	0.479	0.023	-0.241, 0.001, 0.008
cis-HCOOH-ads-G	-0.77	2.237	2.023, 1.993, 1.979	0.531	0.101	-0.204, 0.017, -0.014
cis-HCOOH-ads-H	-0.90	2.333	2.018, 1.998, 1.985	0.546	0.134	-0.174, 0.022, -0.021
cis-HCOOH-ads-I	-0.36	2.196, 2.302	1.984, 1.998, 1.995	0.437	0.079	-0.163, -0.068, 0.010
cis-HCOOH-ads-J	-0.73	2.369	1.971, 1.995, 1.998	0.507	0.127	-0.194, 0.006, 0.014

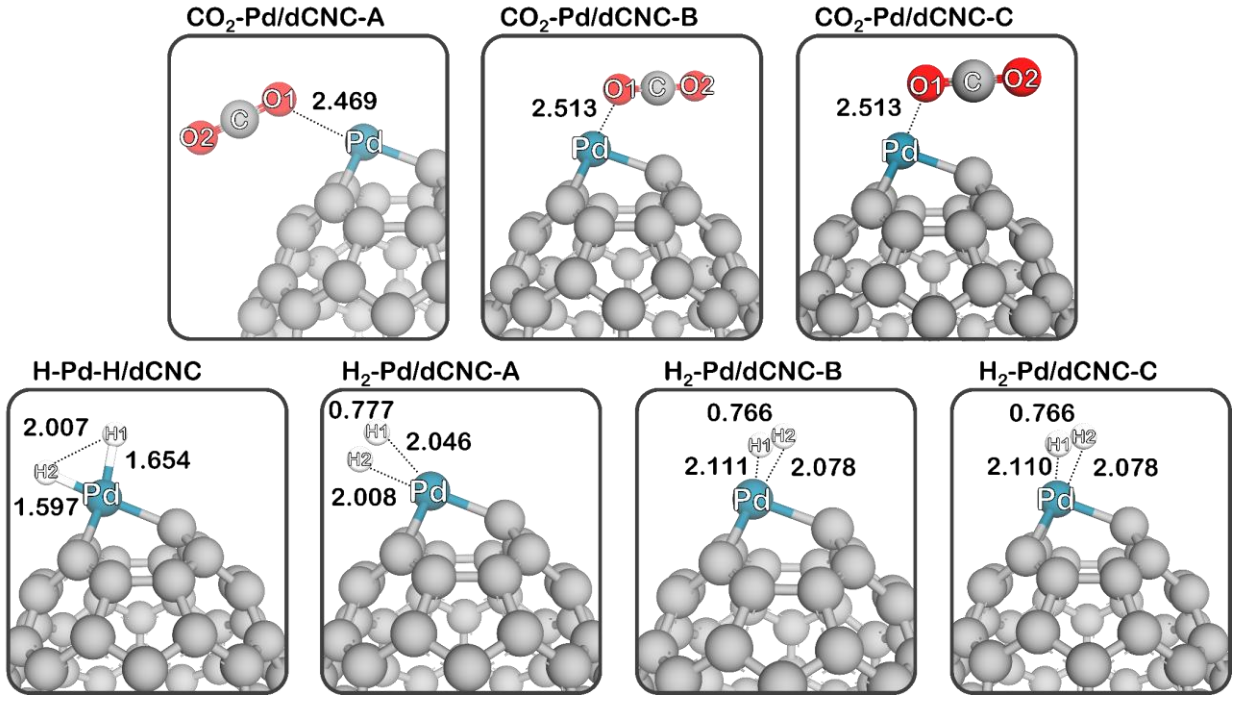

Figure S6 – All stable configurations of H_2, CO_2 adsorption over Pd/dCNC

Table S5 – CO_2 and H_2 adsorption properties of a Pd atom supported dCNC

System	E_{ads}, eV	d(gas-Pd), Å	d(Pd-C), Å	q(Pd)	q(gas)	q(C1, C2, C3)
CO_2-Pd/dCNC-A	-0.42	2.469	1.970, 1.994, 1.994	0.102	0.076	-0.059, 0.001, 0.001
CO_2-Pd/dCNC-B	-0.37	2.513	2.005, 1.980, 1.991	0.131	0.078	-0.092, 0.000, -0.029,
CO_2-Pd/dCNC-C	-0.37	2.513	2.005, 1.991, 1.980	0.131	0.079	-0.091, -0.029, 0.000
H-Pd-H/dCNC	0.16	1.597, 1.654	2.044, 1.993, 1.993	-0.179	0.068	-0.095, -0.004, -0.004
H_2-Pd/dCNC-A	-0.32	2.008, 2.046	1.979, 2.015, 2.015	0.027	0.113	-0.074, -0.031, -0.031
H_2-Pd/dCNC-B	-0.13	2.078, 2.111	2.022, 1.985, 2.005	0.042	0.107	-0.067, -0.010, -0.037
H_2-Pd/dCNC-C	-0.13	2.078, 2.110	2.022, 2.005, 1.985	0.042	0.107	-0.067, -0.037, -0.010

To understand the mechanism of FA dehydrogenation into H_2, the final product should be considered. We first consider the adsorption of individual CO_2 and H_2 products over Pd/dCNC surface by

varying the position and orientation of molecules to verify the most stable configurations. **Figure S6** show all energetically favorable structures for CO_2 and H_2.

For CO_2 adsorption, we found three possible configurations, namely **CO_2-Pd/dCNC-A, B,** and **C**. The structural and electronic properties are demonstrated in **Table S5**. The adsorption energy for **CO_2-Pd/dCNC-A** is -0.42 and -0.37 eV for **B,** and **C** configurations, which is greater than that for adsorption on the perfect CNC surface (-0.13 eV).[3] In addition, the Pd-O intermolecular bond distance of **CO_2-Pd/dCNC-A** is 2.469 Å, and **B,** and **C** configurations have 2.513 Å. For H_2 adsorption, two different types of H_2 adsorption are found for a carbon-based-nanomaterial supported metal atom. These are (*i*) Kubas mode (or K-mode), a non-dissociative H_2 adsorption[4] and (*i*) D-mode, a dissociated dihydride adsorption.[5] In this work for Pd/CNC, we obtain H_2 adsorption either K- or D-mode for clarify the possibility of H_2 production. In the case of K-mode, there are three stable structures with the E_{ads} of -0.32 and -0.13 eV for **H_2-Pd/dCNC-A** and **B, C**, respectively. Interestingly, the adsorption of H_2 in D-mode has 0.16 eV, which is unstable configuration. Therefore, the H_2 production over Pd/dCNC preferentially occur in molecule than that it is in atoms.

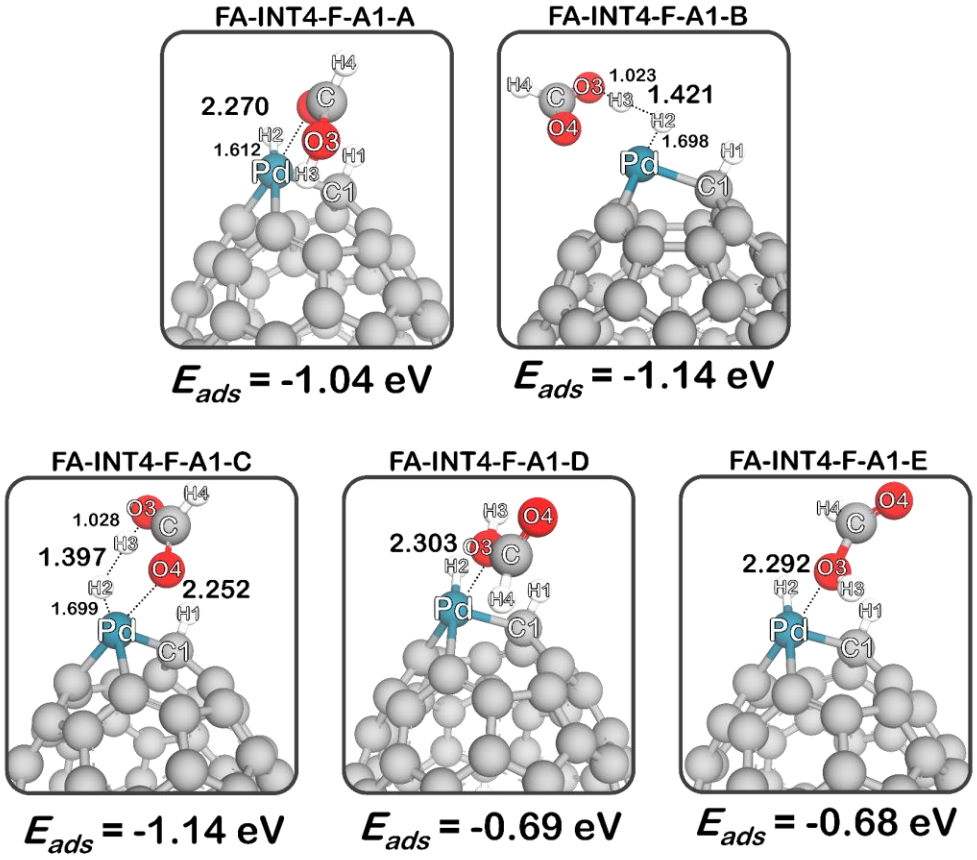

Figure S7 – All stable configurations of 2nd *trans*-FA adsorption over **INT4-F- A1** intermediate.

S3. FA dehydrogenation on Pd/dCNC through a formate intermediate

Route A1

We propose a reaction mechanism for *trans*-HCOOH dehydrogenation via route A1. Following the dehydrogenation of *trans*-HCOOH, the reaction converts FA molecules into H_2 and CO_2 through a formate intermediate. **Figure 3** represents the catalytic reaction pathway and optimized structures for route A1. We set ***trans*-HCOOH-ads-A** as an initial state for dehydrogenation, with relative energy (E_{rel}) of -1.23 eV. At the first transition state, *trans*-HCOOH is dehydrogenated to the C1 atom to generate the bidentate formate (*OOCH) ligand. The intermolecular H1-C1 bond distance shortens from 1.666 Å to 1.541 Å. The calculated activation energy-barrier (E_a) for formate formation is about 0.002 eV, with a single imaginary frequency of -388.38 cm^{-1}. This almost barrierless value is significantly less than the reaction on the Pd/dG material (0.39 eV).[6] The neighboring C1 atom on CNC has very high reactivity, which brings about the small energy barrier in the first step of dehydrogenation. The POAV effect on the curved material can explain this small energy barrier, as described in our previous work.[7] By following the **TS1-F-A1**, the bidentate *OOCH intermediate gains an E_{rel} of -2.32 eV. We studied the **TS2-F-A1** to investigate the second dehydrogenation in which the bidentate *OOCH ligand converts to its monodentate form. This step has an energy barrier of approximately 0.82 eV. The monodentate OOCH ligand forms with an E_{rel} of around -1.60 eV. Next, the H2 migrates to the Pd atom with an E_a value of 0.54 eV. The single imaginary frequency is -490.90 cm^{-1}. The distance between C and H2 increases to leave a Pd hydride on the catalyst and produces a CO_2 molecule. The CO_2 then desorbs from the Pd/dCNC with an energy of 0.35 eV. In the final step, H_2 must form. We classify the process into two possible pathways. The first pathway starts with H2 migration from one side to the other to create an available site for the upcoming H1 atom.

This step has an energy barrier of 0.29 eV with a single imaginary frequency of -446.74 cm^{-1}. The H1 migration step from C1 to a Pd atom has very high E_a (1.81 eV), which is the RDS for route A1. Frequency calculations reveal one imaginary frequency of -856.91 cm^{-1}. The H1-H2 then forms spontaneously with a bond distance of approximately 1.408 Å. The H_2 formation has an energy barrier of only 0.09 eV and uses a single imaginary frequency of -768.40 cm^{-1}. Next, the H_2 molecule adsorbs onto Pd/dCNC by physisorption with an E_{ads} of -0.31 eV. Another H_2 formation is found (blue line in **Figure 3**). Route A1-ver2 starts with **INT4-F-A1.** The two deposited H atoms directly form an H_2 molecule, with a slightly higher energy barrier of 1.52 eV. The single imaginary frequency is -1512.29 cm^{-1}. We conclude that the C1-H1 bond cleavage is very difficult on Pd/dCNC, as evidenced by the high E_a of **TS5-F-A1** and **TS5-F-A1-ver2.**

To decrease the RDS, we created a new pathway for FA dehydrogenation by adding a second *trans*-FA to **INT4-F-A1**. We find the most stable FA adsorption (**Figure S7)** occurs when the hydroxyl group of the second *trans*-FA attaches to a deposited H on a Pd atom and the carbonyl oxygen points directly to the Pd atom. The calculated E_{ads} of **HCOOH-INT4-F-A1** is -1.14 eV. The dehydrogenation of 2nd *trans*-FA to form H_2 requires an energy barrier of only 0.11 eV. There is an associated imaginary frequency of -958.80 cm^{-1} associated with **TS4-F-A1-ver3**. So, the RDS of this desired reaction is 0.82 eV, indicating the formation of monodentate OOCH. In summary, we suggest that H_2 production through FA dehydrogenation over Pd/dCNC would occur following the second FA dehydrogenation, rather than by direct H_2 formation from a deposited H-atom at C1. When H_2 is released, the catalytic component is similar to **INT1-F-A1**, providing a catalytically active site for FA dehydrogenation in its second cycle.

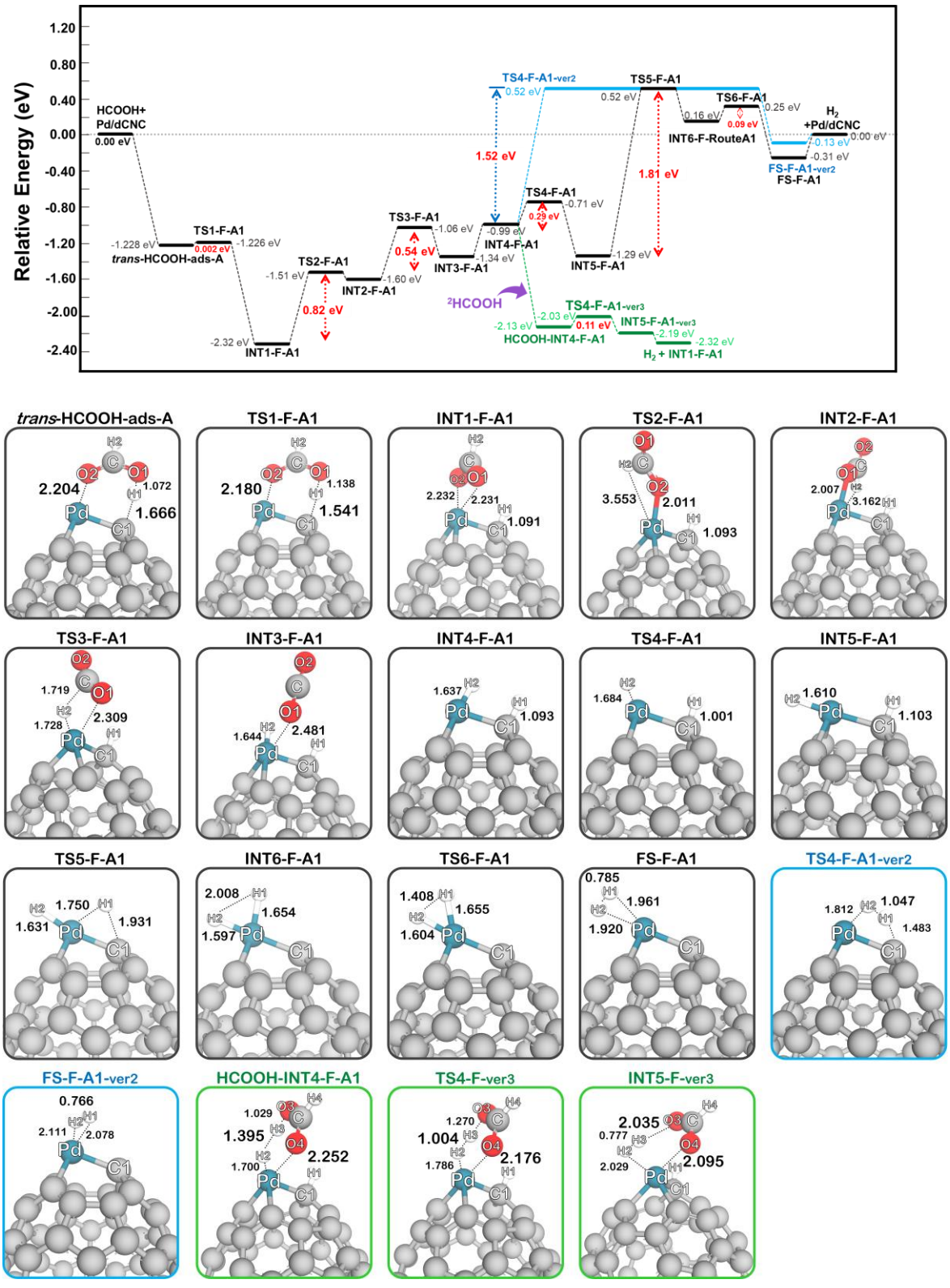

Figure S8 – Energy profile showing optimized initial-state, transition state, and final state

geometries for *trans*-HCOOH dehydrogenation over Pd/dCNC via the formate pathway (Route A1). All distances are in Å.

Route A2

Route A2 is one possible reaction mechanism to progress via formate species. The initial state for ***trans*-HCOOH-ads-D** has an E_{ads} value of -0.77 eV. This adsorption mode requires that either carbonyl oxygen or a hydroxyl group attaches to a Pd atom. At the first transition state, the H1 dehydrogenates with an elongation of the O1-H1 bond from 0.981 Å to 1.639 Å. The E_a is 0.91 eV, which is higher than that of the first H dehydrogenation in route A1. After the dehydrogenation of adsorbed HCOOH, the produced HCOO* intermediate will undergo a ligand rotation step via **TS2-F-A2,** to transform to **INT2-F-A2** with a low barrier of 0.02 eV. The 2nd dehydrogenation takes place via **TS3-F-A2** by overcoming the energy-barrier of 0.20 eV. **TS3-F-A2-ver2** is another possible second H-dehydrogenation to produce H_2 directly. However, the activation energy is too high (1.11 eV). Thus, direct H_2 production from the HCOO* intermediate is negligible. The CO_2 molecule sequentially desorbs from Pd/dCNC with desorption energy of 0.45 eV. Then, the 2H* on Pd or **H-Pd-H/dCNC** has a longer H-H distance of 2.008 Å compared to the bond length of H_2 of about 0.74 Å. The significant energy barrier of the H_2 formation reaction on Pd/dCNC is only 0.09 eV, with a single imaginary frequency of -768.40 cm^{-1}. Also, the desorption energy of H_2 is only -0.31 eV, which confirms the preference for H_2 production. This remarkable result confirms that the Pd/dCNC catalyst favors H_2 production. Our results show that the RDS in *trans*-HCOOH dehydrogenation over Pd/dCNC catalyst via formate pathway (Route A2) has 0.91 eV. From our study, the dehydrogenation to Pd atom, without a deposited H on neighboring carbon, is slightly more difficult compared to **TS3-F-A1** (0.54 eV).

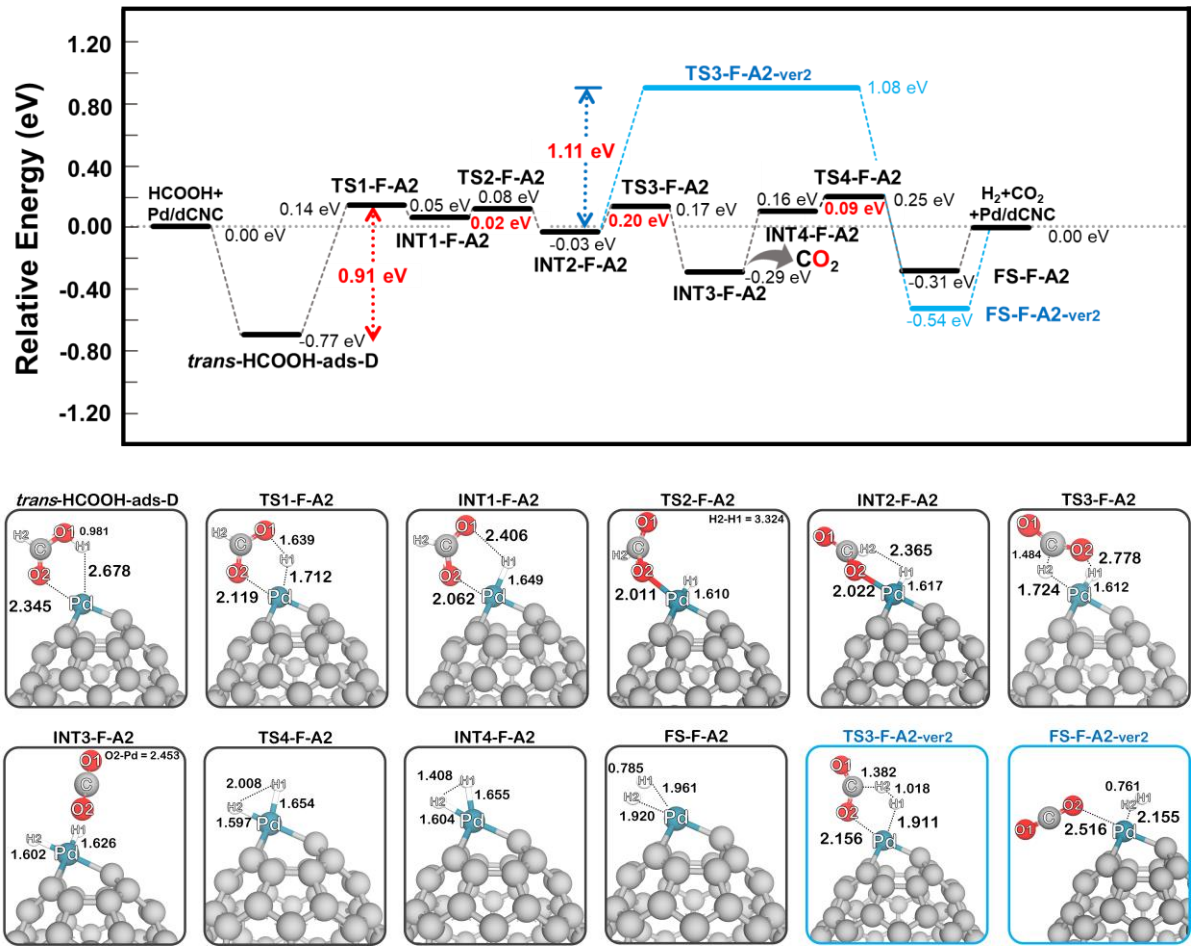

Figure S9 – Catalytic reaction pathway of *trans*-HCOOH dehydrogenation over Pd/dCNC catalyst via formate pathway (Route A2). All distances are in Å.

Route A4

For route A4, the potential energy surface (PES) of *cis*-FA dehydrogenation has been computed and mapped (**Figure 7**). The initial state is with *cis*-FA orienting to Pd/CNC by the hydroxyl oxygen with an O-Pd distance of 2.369 Å and adsorption energy of -0.73 eV. The *cis*-FA dissociates its hydroxyl H-atom, and sequentially forms co-adsorbed H* and monodentate HCOO*. **TS1-F-A4** is the transition state structure, in which O1-H1 and H1-Pd bond distances are 1.443 Å and 1.620 Å, respectively. Pd/dCNC gives a slightly higher barrier for the first dehydrogenation via route A4, with an E_a of 1.65 eV, which is the RDS of route A4. The

calculated single imaginary frequency is -1104.63 cm^{-1}. The first dehydrogenation is more difficult when the reaction starts without a deposited H on the neighboring C atom and is virtually indistinguishable from the same step in route A2. Following the **INT1-F-A4,** the H2 atom deprotonates from the Pd atom. The bond distance between C-H2 lengthens from 1.111 to 1.567 Å, with an E_a of 0.22 eV, and an imaginary frequency of -488.52 cm^{-1}. The CO_2 forms with relative energy of -0.51 eV. H_2 formation occurs after CO_2 desorption. We find that the H_2 formation occurs easily, by a similar process, as described for route A2.

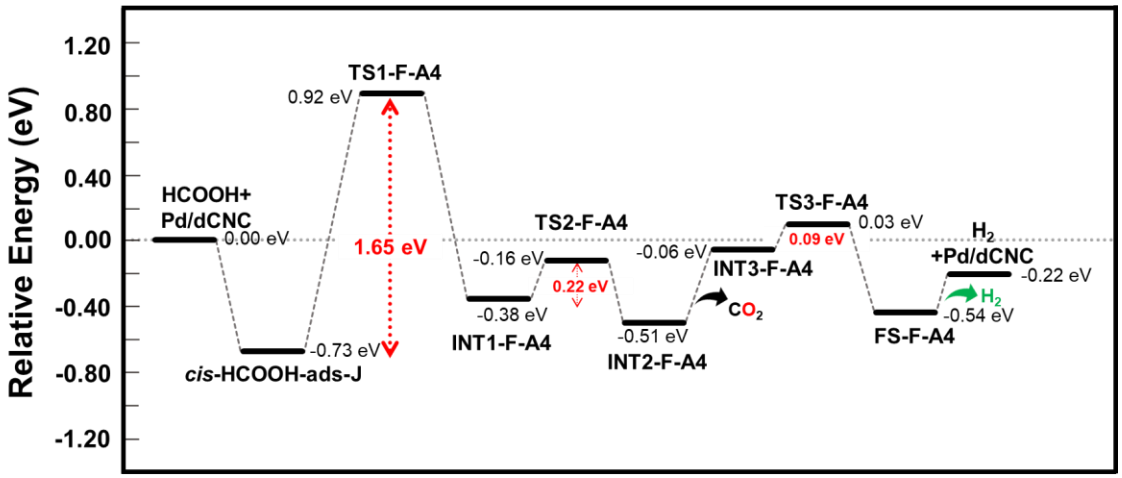

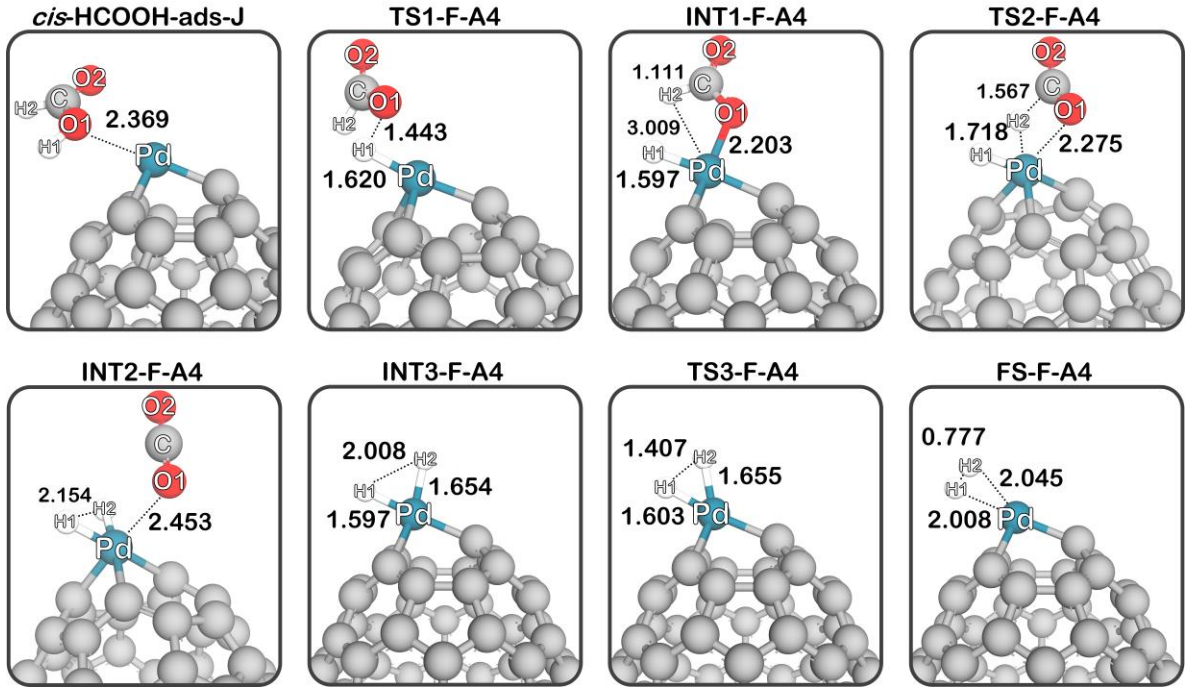

Figure S10 – Reaction mechanism of *cis*-HCOOH dehydrogenation over Pd/dCNC catalyst via formate pathway (Route A4). All distances are in Å.

Route A6

The catalytic cycle for the formation of H_2 from FA over Pd/dCNC via route A6 (**Figure 6c**) is similar to route A5 but occurs at a different site. This process starts from ***cis*-HCOOH-ads-I** and converts into **TS1-F-A6** by dehydrogenation of H1 at C2. The energy barrier of this step is exothermic, at 0.62 eV. The *cis*-FA attached to either Pd or C2 at the active site undergoes H migration to the active C2 atom. At **TS1-F-A6**, the H1-C2 and H2-Pd bond lengths are 1.384 Å and 1.958 Å, respectively. The calculated single imaginary frequency is -1640.76 cm^{-1}. The monodentate formate ligand forms with an E_{rel} of -1.22 eV and a Pd-O bond length of 2.001 Å, which is relatively stable. Direct H_2 formation from H1 and H2 is prohibited because of the high E_a value of 1.91 eV (blue line **Figure 9**). The second dehydrogenation, to the Pd atom, happens with a small energy barrier of 0.48 eV.

Next, CO_2 desorption yields **INT3-F-A6**. To reduce the E_a of H_2 formation, the second *cis*-FA adsorbed on **INT3-F-A6** with the E_{ads} of -0.46 eV. The energy barrier to H_2 production is 0.51 eV, with a single imaginary frequency of -701.01 cm^{-1}, which is in good agreement with H_2 formation via the second FA, as described in the previous route. At **TS3-F-A6**, the synchronic activation of C-H4 and O3-H3 generates the CO_2 and H_2. After their release, a third *cis*-FA molecule adsorbs on to **INT6-F-A6** to complete the cycle, with an E_{ads} of -0.43 eV. This step is identical with dehydrogenation of the second *cis*-FA. The adsorbed *cis*-FA simultaneously dissociates its two H atoms of the hydroxyl (O5-H5) and the C-H6 group, with an E_a of 0.57 eV, and a single imaginary frequency of -712.41 cm^{-1}. The catalyst is similar to **INT3-F-A6** after releasing H_2 and CO_2 and opens an active site for the second cycle of *cis*-FA dehydrogenation. The RDS of *cis*-FA dehydrogenation via route A6 is 0.62 eV. Therefore, the dehydrogenation of H1 to C1 is easier than it is to C2. Dehydrogenation to C1 has an energy barrier of only 0.19 eV, as mentioned for route A5 and FA adsorption energies explained this behavior. The E_{ads} of ***cis*-HCOOH-ads-I** is -0.36 eV, which is slightly smaller than ***cis*-HCOOH-ads-F** (-0.51 eV). Moreover, we found that the C2-H1 bond distance in ***cis*-HCOOH-ads-I** is longer than the C1-H1 for ***cis*-HCOOH-ads-F**. The structural, electronic, and energetic properties confirm a higher E_a for route A6 rather than route A5. Consequently, the *cis*-FA dehydrogenation via route A5 is the preferred reaction path.

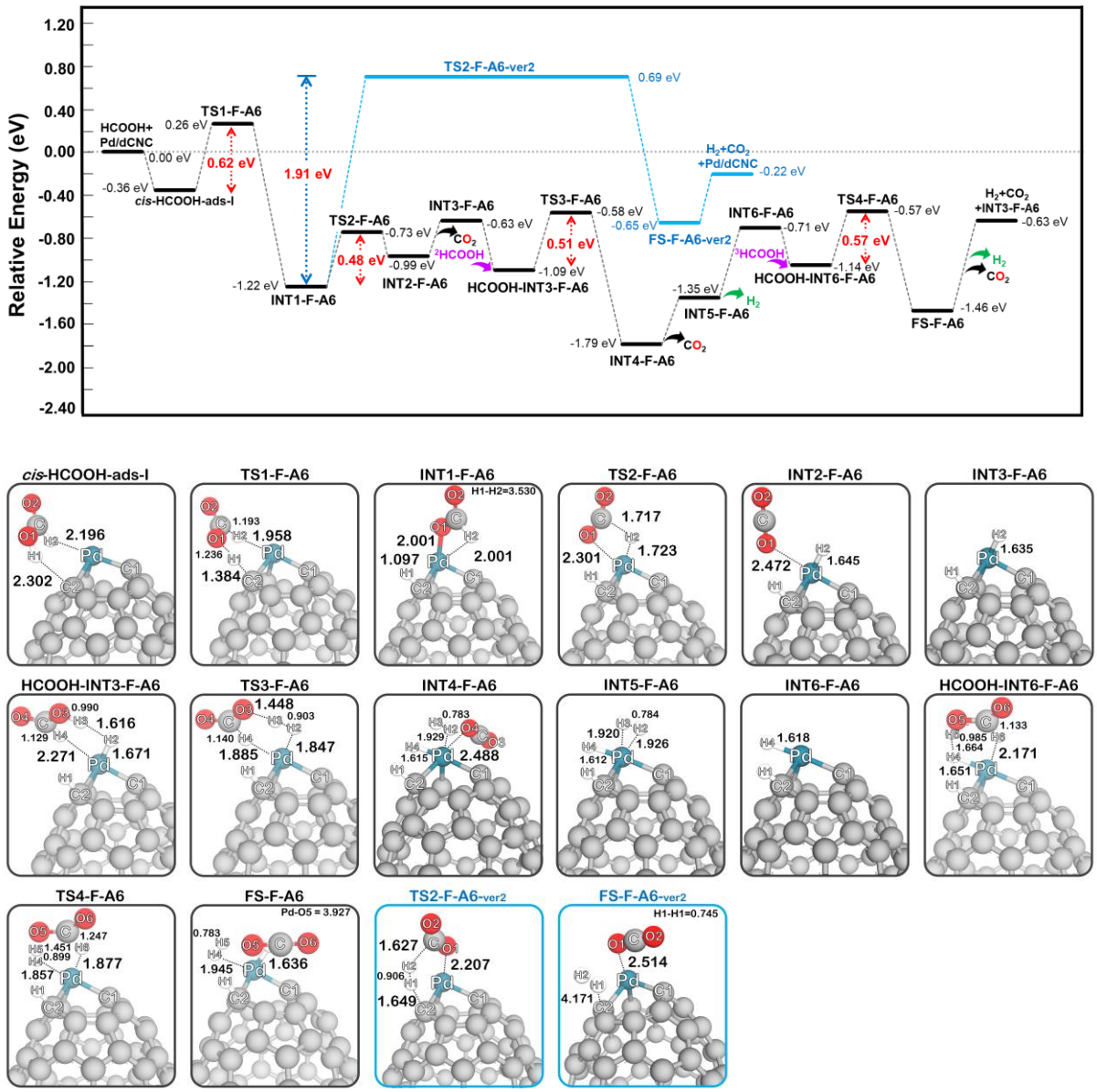

Figure S11 – Reaction mechanism of *cis*-HCOOH dehydrogenation over Pd/dCNC catalyst via the formate pathway (Route A6). All distances are in Å.

S4. FA dehydrogenation on Pd/dCNC through a carboxyl intermediate

Route B1 and B2

In this section, we attemp to discuss the *trans*-FA dehydrogenation reaction via carboxyl pathway. We proposed three possible reaction pathways; a. route B1, b. route B2, and c. route B3 representing the different adsorption configurations.

Route B1 starts with ***trans*-HCOOH-ads-B** configuration. Then, the C-H2 bond is cleavage on Pd/dCNC with an energy barrier of 1.26 eV (see **Figure S13**). The single imaginary frequency of **TS-C-B1** is -597.33 cm^{-1}. The carboxyl intermediate is formed with C-H1 bond lengthens from 1.586 to 2.521 Å. This step is an endothermic reaction. To get a suitable configuration for the second dehydrogenation of COOH*, the carboxyl ligand is rotated with a requirement energy barrier of 1.50 eV. The final state of this step is **INT2-C-B1**. Following **INT2-C-B1** intermediate, there are two possible reaction paths for the 2^{nd} dehydrogenation. The first pathway is direct H_2 formation via O1-H1 breaking and H1-H2 forming with a small energy barrier of 0.07 eV. The single imaginary frequency of **TS3-C-B1** is calculated to be -1129.43 cm^{-1}. The second pathway is the mechanism of the dehydrogenation of H1 to Pd atom to form the CO_2 molecule. This step required E_a of 0.51 eV. The CO_2 is then desorbed from the surface. Finally, the H_2 is generated by forming deposited H1 and H2 atoms through energy barrier of only 0.09 eV, with the single imaginary frequency of -769.76 cm^{-1}. Therefore, the rate determining step of dehydrogenation via carboxyl is found to be 1.50 eV in the step of COOH* rotation.

Moreover, we consider another orientation of carboxyl intermediate as defined in route B2. This reaction mechanism is similar to route B1, but the OH group of carboxyl ligand orients in different direction. In the route B2, the pointed in hydroxide is found as **INT1-C-B2**. From our

calculation, we found that the reaction mechanisms of route B1 and B2 are the same in terms of relative energies and activation energy barrier. So, we would not discuss route B2 in the details.

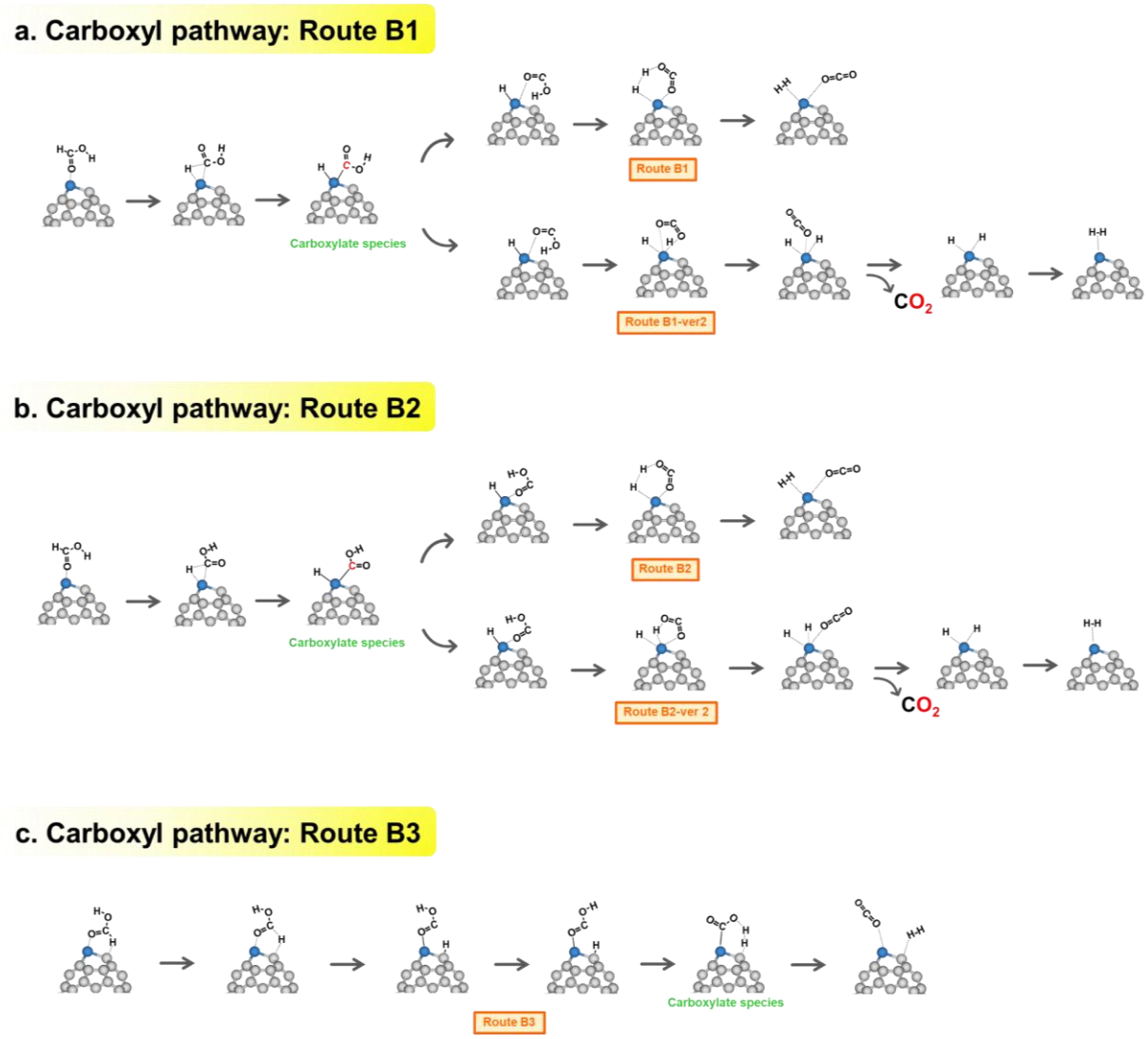

Figure S12 – Proposed catalytic reaction pathways for *trans*-HCOOH dehydrogenation over Pd/dCNC catalyst via carboxylate intermediate.

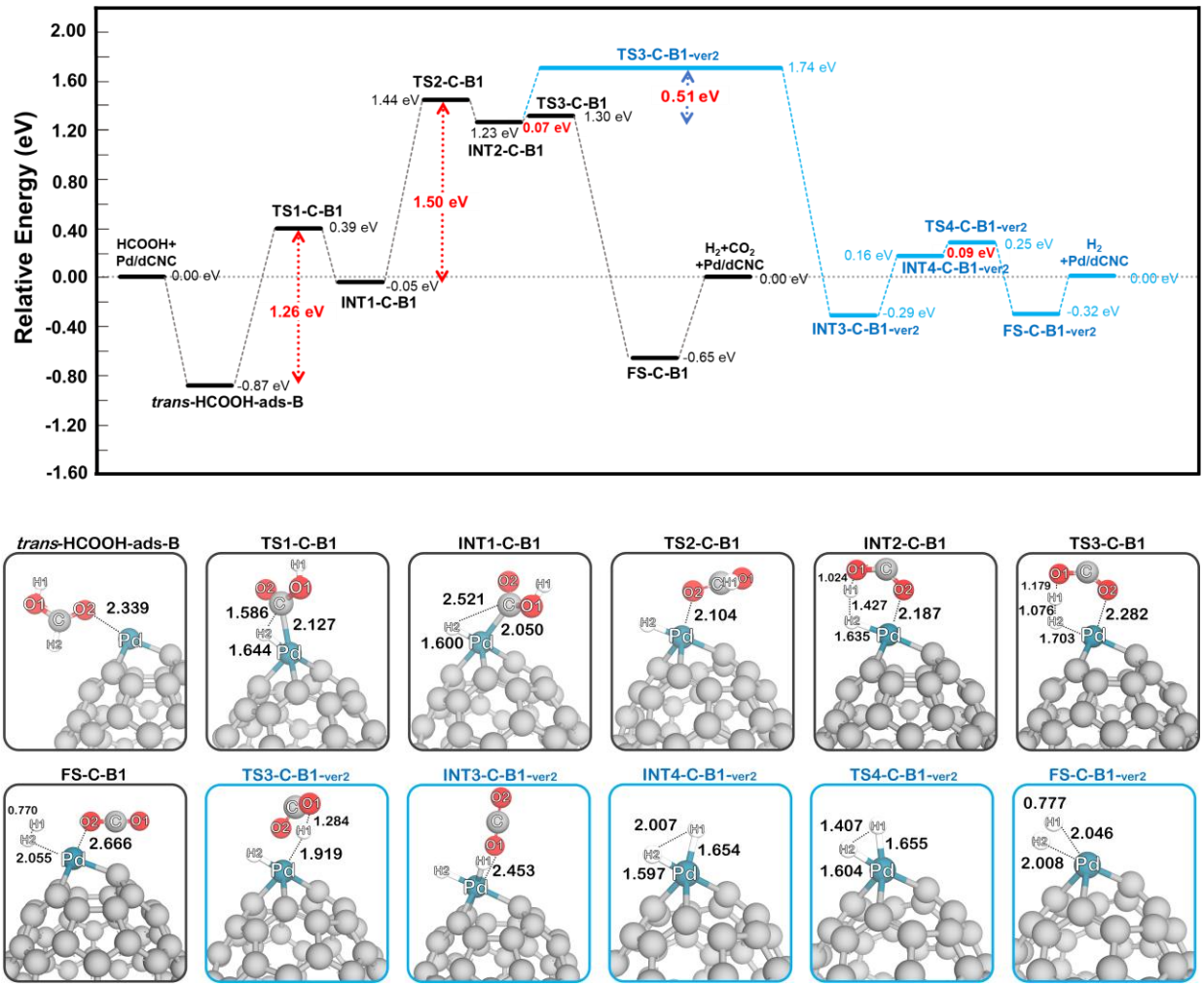

Figure S13 – Reaction mechanism of *trans*-HCOOH dehydrogenation over Pd/dCNC catalyst via carboxyl pathway (Route B1). All distances are in Å.

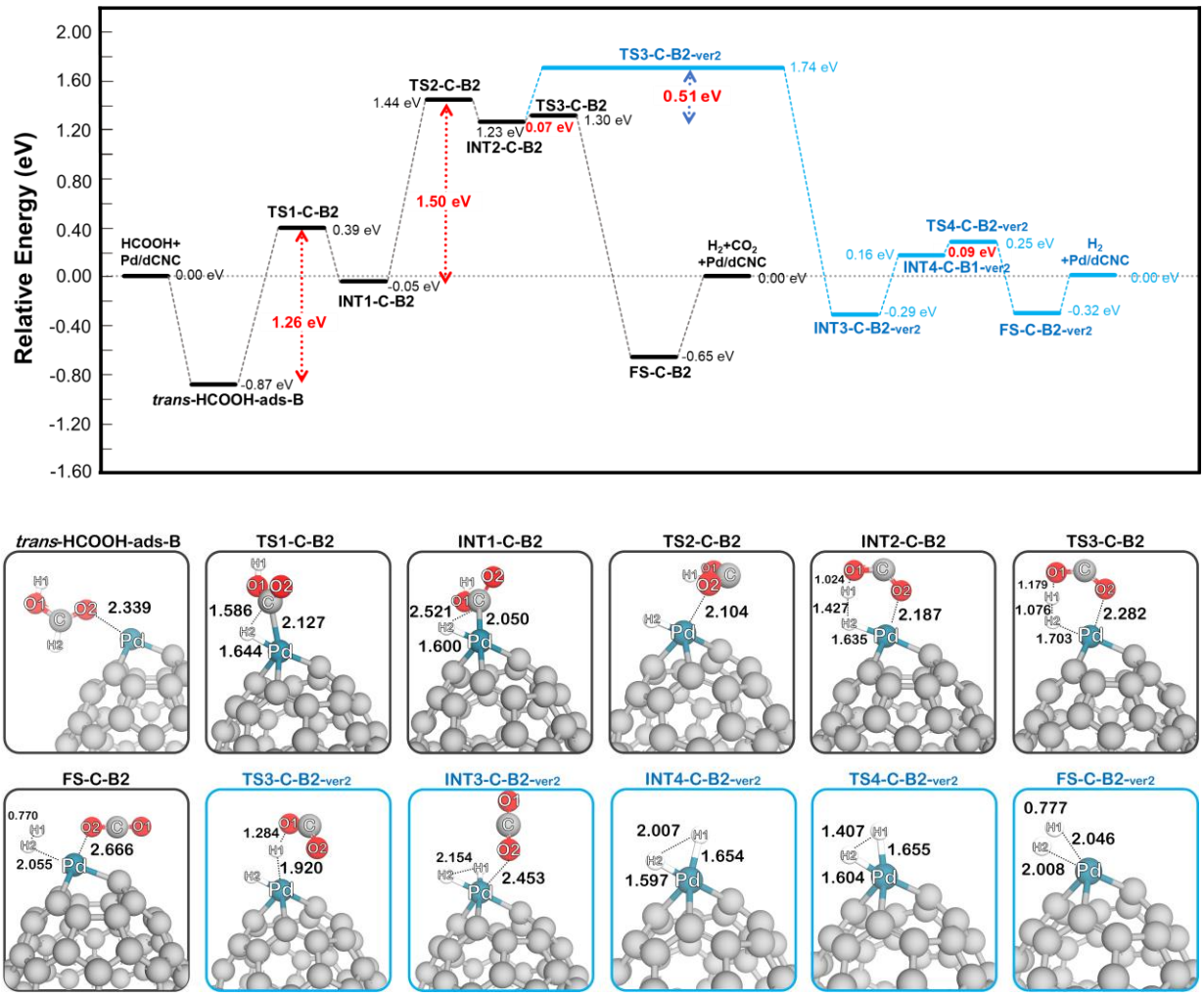

Figure S14 – Reaction mechanism of *trans*-HCOOH dehydrogenation over Pd/dCNC catalyst via carboxyl pathway (Route B2). All distances are in Å.

Route B4 and B6

Next, we study the *cis*-FA dehydrogenatio reaction via carboxyl intermediate. Three possible reaction mechanisms are found; a. route B4, b. route B5, and c. route B6 represent the different adsorption configurations as showed in **Figure S15**.

We first consider the reaction of dehydrogenation via route B4. **Figure S16** demonstrates the energy profile and the structures along the reaction pathway. ***cis*-HCOOH-ads-B** is set as an initial state for the reaction with the adsorption energy of -0.92 eV. Then, at the first transition

state, the C-H2 is cleavage to form carboxyl intermediate, with a single imaginary frequency of -595.62 cm^{-1}. The requirement energy barrier is 1.17 eV. The H and *COOH co-adsorption are found to be **INT1-C-B4** with the H2-Pd and C-Pd bond distance of 2.515 and 2.042 Å, respectively. Following the **INT1-C-B4**, the O1-H1 bond dissociates to form H_2 molecule with the E_a of 1.18 eV, which is the RDS of the reaction. Then, CO_2 and H_2 are co-adsorbed on Pd/dCNC with E_{ads} of -0.87 eV. Moreover, we found another possible dehydrogenation pathway, that the H1 atom dehydrogenates to Pd atom to yield the CO_2 instead of direct H_2 formation (illustrated in blue line of **Figure 16**). The E_a is calculated to be 1.99 eV, with a single imaginary frequency of -1837.93 cm^{-1}. After that, adsorbed CO_2 is then desorbed from the H-Pd-H, and H_2 production happen after CO_2 desorption with a small E_a of 0.09 eV. Compared to route B5, the reaction mechanism is almost the same with route B5 in terms of relative energies and activation energy barrier, but the OH group of carboxyl ligand orients in different direction. Hence, we discussed in the details only route B5 in the main manuscript.

In addition, the reaction of *cis*-FA dehydrogenation via carboxyl is also investigated via route B6. We propose the reaction mechanism by starting with ***cis*-HCOOH-ads-H.** The dehydrogenated H of cis-FA is facilitated with an energy barrier of 0.96 eV. There is an associated imaginary frequency of -1443.56 cm^{-1} associated with transition state **TS1-F-B6**, and form *OCOH ligand. Next, the hydrogen production occurred via H1-H2 forming at **TS2-C-B6**, with the activation energy of 1.20 eV. The calculated single imaginary frequency is -929.18 cm^{-1}. Then, co-adsorbed H_2 and CO_2 releasing occurs via the use energy of 0.69 eV. Our results reveal that the reaction mechanism over Pd/dCNC via carboxyl pathway (route B6) has the rate determining step of 1.20 eV.

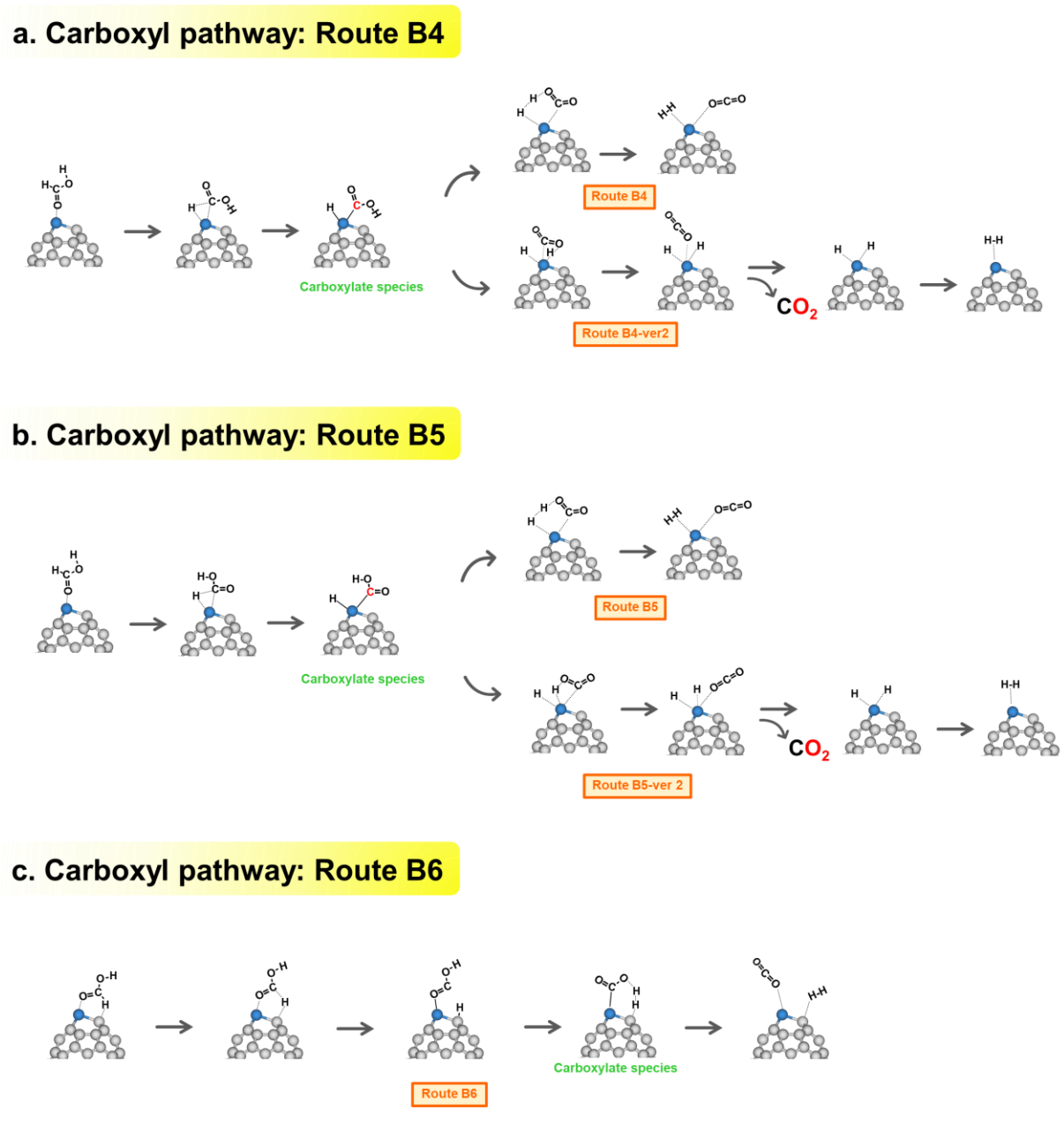

Figure S15 – Proposed catalytic reaction pathways for *cis*-HCOOH dehydrogenation over Pd/dCNC catalyst via carboxylate intermediate.

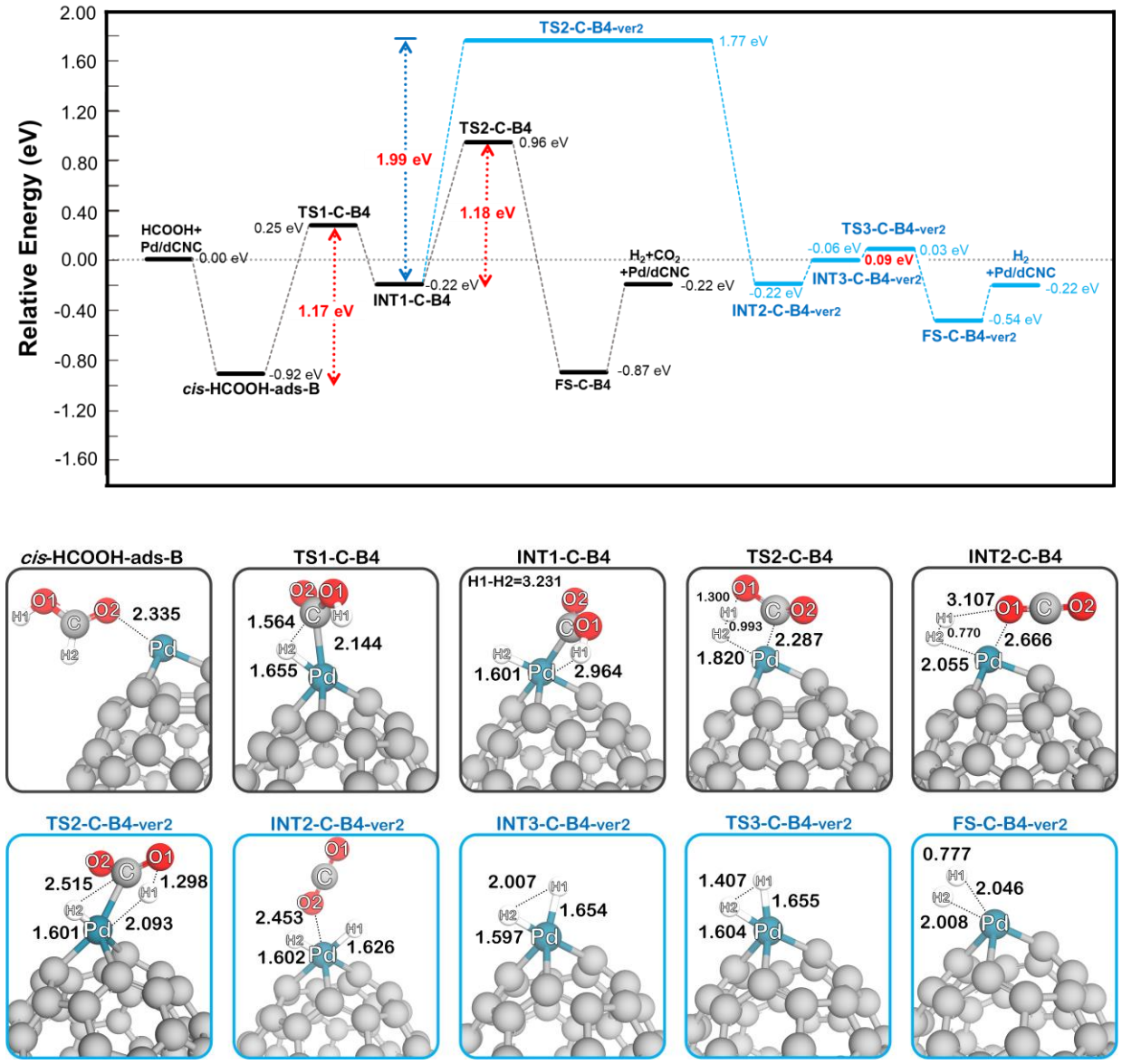

Figure S16 – Reaction mechanism of *cis*-HCOOH dehydrogenation over Pd/dCNC catalyst via carboxyl pathway (Route B4). All distances are in Å.

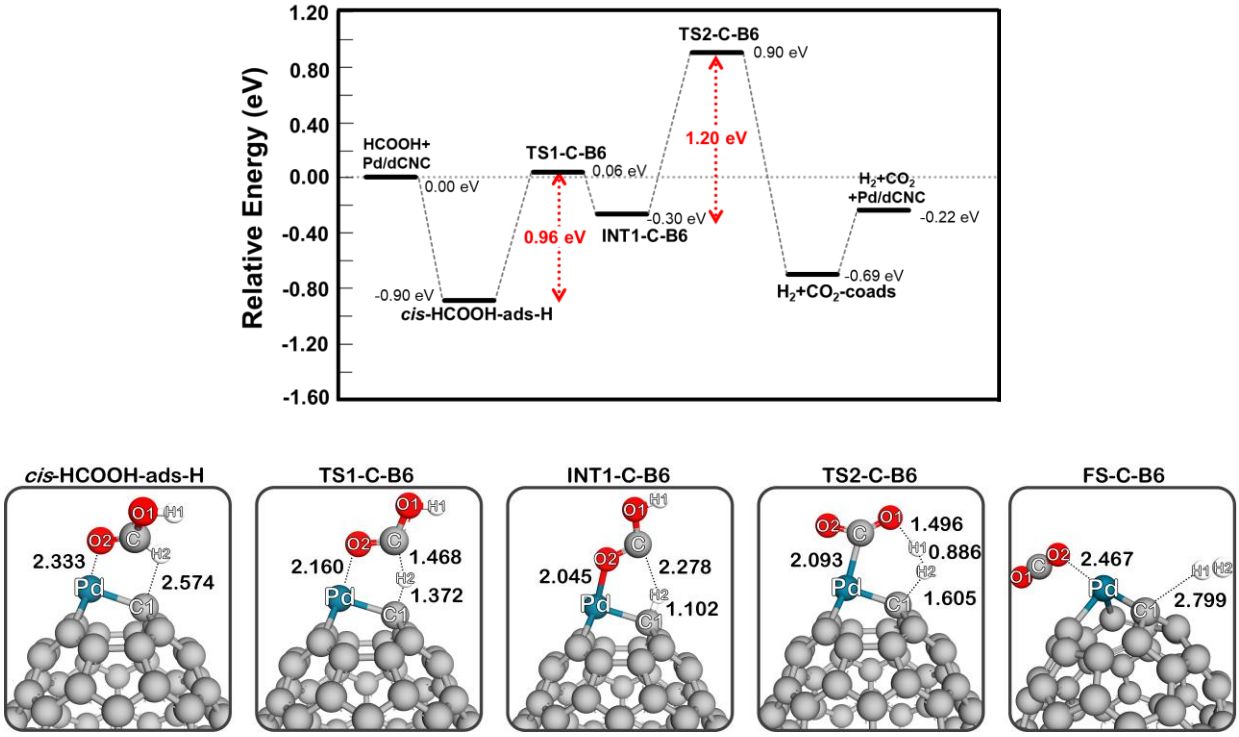

Figure S17 – Reaction mechanism of *cis*-HCOOH dehydrogenation over Pd/dCNC catalyst via carboxyl pathway (Route B6). All distances are in Å.

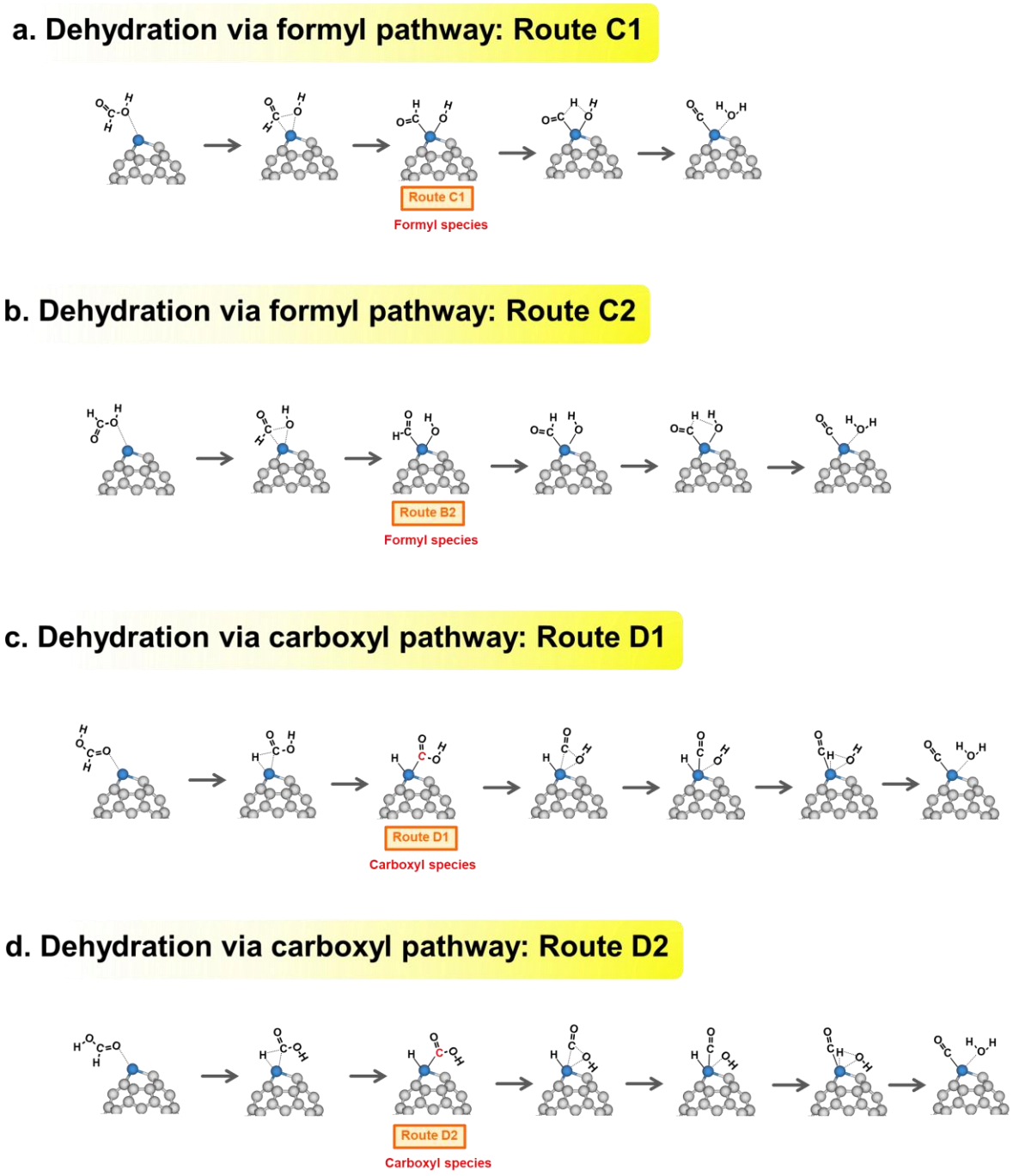

Figure S18 – Proposed catalytic reaction pathways for HCOOH dehydration over Pd/dCNC catalyst via formyl and carboxylate intermediate.

S4. Microkinetic simulations

We investigated microkinetic modelling to achieve overall rates of reactions and product distributions, as well as to predict the catalyst for optimal reactivity in the desired FA dehydrogenation, yielding H_2. In addition, the temperature effect on overall *trans*-FA consumption rates are performed. **Figure S19** illustrated surface coverage by reaction intermediates as a function of temperature, during either *trans*-FA dehydrogenation or dehydration. For the dehydrogenation, we have performed the reaction via both of formate (A1, A3) and carboxyl (B3). Form the result, there is no *trans*-FA molecules on active site because the energy barrier of this step is almost barrierless to yield of bidentate formate intermediate (HCOOb) and a deposited H (H*). So, it is readily to generate HCOOb ligand. The HCOOb mainly occupy on active sites until the temperature reach around 900 K. Owing to the large binding strength of HCOOb ligand, the reaction would occur at around 900 K, which might result in the production of CO rather than that of H_2. Then HCOOb* coverage declines rapidly with increasing temperature from 800−1000 K. It is critical regarding the CO production and the subsequent possibility of poisoning. In the case of the reaction via route A3, it is similar to route A that the HCOOb* and H* are automatically happen when the first FA is adsorbed on Pd/dCNC. The adsorbed the HCOOb* mainly reside on catalyst until the temperature reach 300 K, see **Figure S19b**. When the temperature reaches 550 K, the coverage of HCOOb* ligand and H* atom declines dramatically with the increasing from 300 to 550 K. For the second FA, the Pd/dCNC is covered by 2^{nd} FA until 400 K. The FA completely vanished at 400 K to yield hydrogen molecule. Overall process, the RDS of the reaction via route A3 is conversion of bidentate to monodentate formate. The microkinetic analysis provides that, after 550 K, HCOOb* coverage is consumed, the adsorbed HCOOb* can be completely converted to HCOOm*. Therefore, at the remarkably lower temperature, FA dehydrogenation via route A3 is more likely

than that of via route A1, with a low RDS of 0.50 eV, it provides the dominant reaction pathway.

Moreover, to confirm that FA dehydrogenation via formate is more preferable rather than it is carboxyl, the microkinetic model of the reaction via carboxyl path is also investigated as depicted in **Figure S19c**. From the result, we found that there is no species coverage on the Pd/dCNC. The gas production from **Figure S20c** suggests that FA dehydrogenation via carboxyl would be occurred at very high temperature. Thus, we strongly sure that the hydrogen production via FA dehydrogenation preferably proceeds via formate intermediate rather than that of carboxyl.

To confirm the selectivity of Pd/dCNC catalyst, we have performed the *trans*-FA dehydration through formyl (route C1) and carboxyl (route D1). The *trans*-FA* mainly located Pd/dCNC site until the temperature reach 200 K, the adsorption of FA rapidly decreases and disappear at 300 K and 250 for route C1 and D1, respectively. The vanished FA on the catalyst means that they desorb from the surface because there are not any product at temperature range of 200-300 K. Accordingly, the FA dehydration over Pd/dCNC is not only energetically non-feasible but also kinetically unfavorable for the formation of CO as a by-product, confirming selectivity toward H_2 production by our proposed reaction mechanisms on Pd/dCNC.

Figure S20 shows plots of production rate for trans-FA decompositions on the Pd/dCNC catalyst as a function of temperature. The rates and optimal temperatures for the decomposition of FA are slightly different for compared five reaction mechanisms. The FA dehydrogenation possess the greatest H_2 production rate under the lowest temperature regions, with a maximum rate at 350 K for hydrogen production and at 410 K for CO_2 production, which is lower than previous work[8]. The optimal temperature for the reaction via route A1 is approximately 900 K. In addition, the competitive reactions require a very high temperature. Therefore, FA dehydrogenation via route A3, with an electronic energy adsorption of 0.50 eV, gives the best activity than dehydration does, and thus is the dominant reaction mechanism.

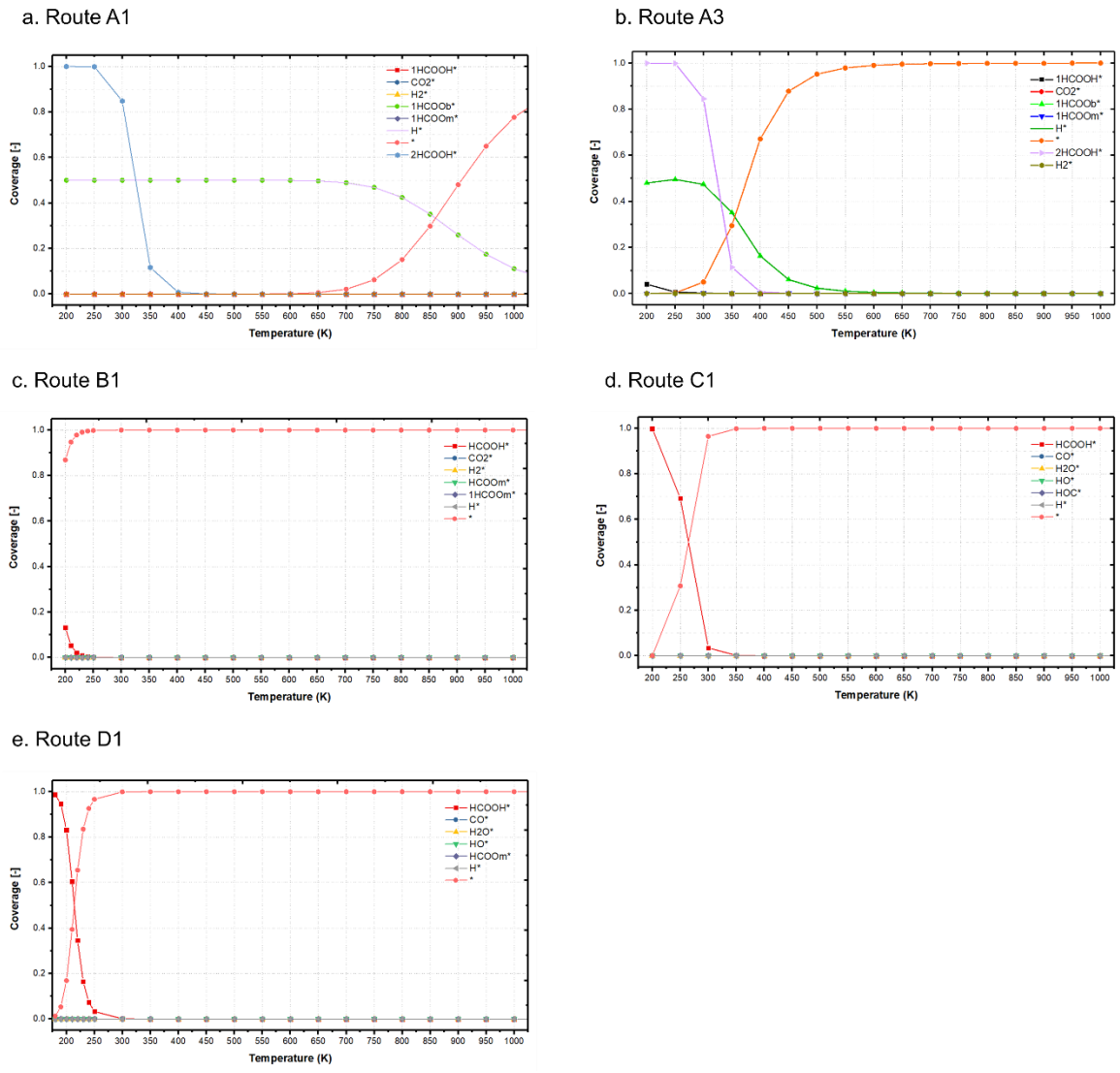

Figure S19 - Surface coverage by intermediates as a function of temperature, for FA decomposition via a) Route A1, b) Route A3, c) Route B3, d) Route C1, and e) Route D1.

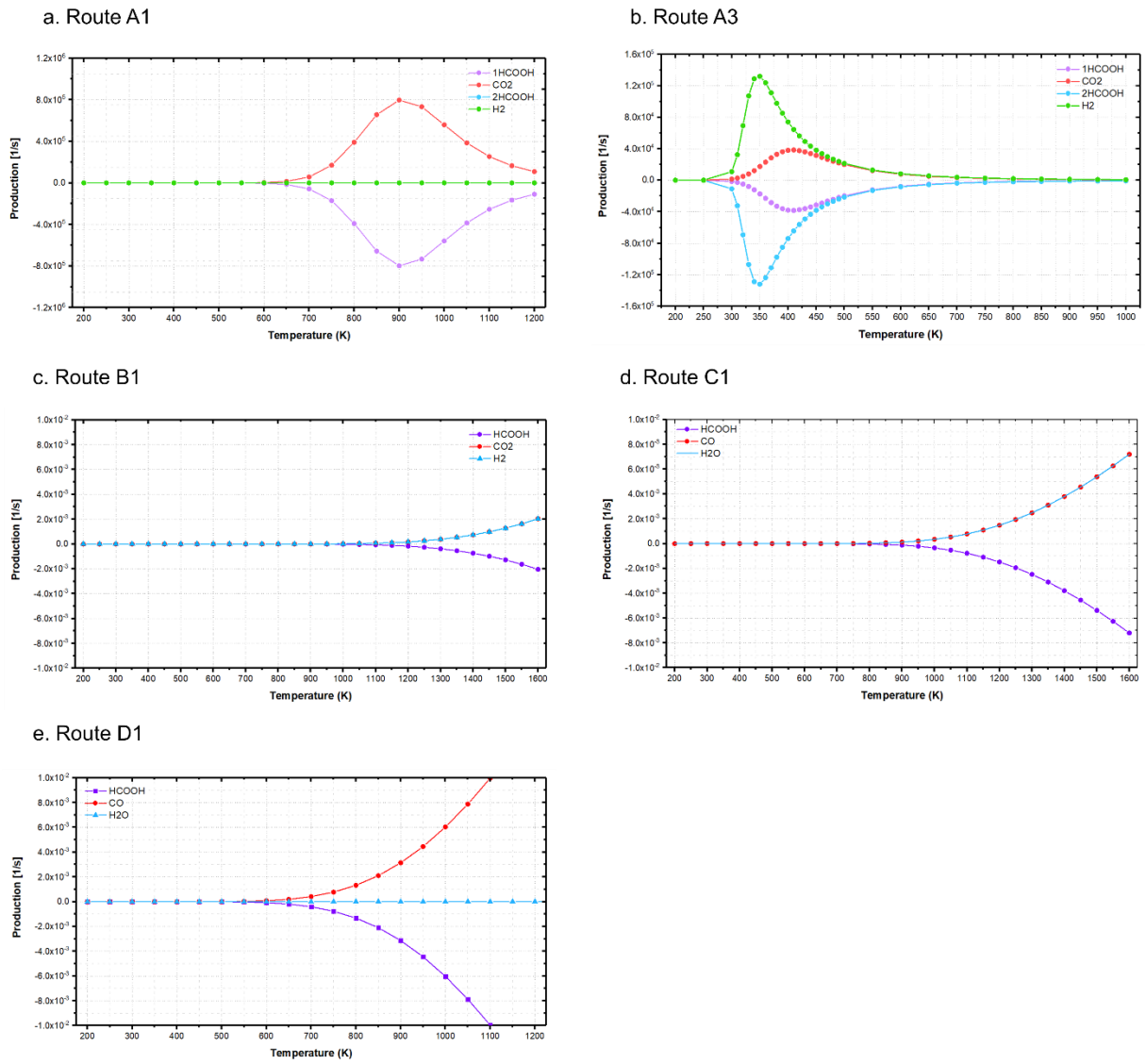

Figure S20 H_2, CO_2, CO, and H_2O production as a function of temperature during FA decomposition via a) dehydrogenation and b) dehydration mechanisms on an Pd/dCNC catalyst.

References

1. L. Ma, J.-M. Zhang, K.-W. Xu and V. Ji, *Applied Surface Science*, 2015, **343**, 121-127.
2. M. D. Esrafili, P. Nematollahi and R. Nurazar, *Superlattices and Microstructures*, 2016, **92**, 60-67.
3. N. Yodsin, C. Rungnim, S. Tungkamani, V. Promarak, S. Namuangruk and S. Jungsuttiwong, *The Journal of Physical Chemistry C*, 2020, **124**, 1941-1949.
4. G. J. Kubas, *Accounts of Chemical Research*, 1988, **21**, 120-128.
5. H. Valencia, A. Gil and G. Frapper, *The Journal of Physical Chemistry C*, 2015, **119**, 5506-5522.
6. Q. Luo, W. Zhang, C.-F. Fu and J. Yang, *International Journal of Hydrogen Energy*, 2018, **43**, 6997-7006.
7. N. Yodsin, C. Rungnim, V. Promarak, S. Namuangruk, N. Kungwan, R. Rattanawan and S. Jungsuttiwong, *Physical Chemistry Chemical Physics*, 2018, **20**, 21194-21203.
8. O. Sneka-Płatek, K. Kaźmierczak, M. Jędrzejczyk, P. Sautet, N. Keller, C. Michel and A. M. Ruppert, *International Journal of Hydrogen Energy*, 2020, **45**, 17339-17353.